SEMARAK ILMU PUBLISHING

Semarak International Journal of Material Research

Journal homepage:
https://semarakilmu.my/index.php/sijmr/index
ISSN: 3083-8908

Experimental and Finite Element Analysis of Multi Layers Composite Materials for Wind Turbine Blade under Aerodynamic Loads

Eslam Shamso[1,*], Medhat El-Hadek[1], Samar Elsanabary[1], Rasha M. Soliman[1], Abla El-Megharbel[1]

[1] Production Engineering and Mechanical Design Department, Faculty of Engineering, Port-Said University, Port Fouad City, Port Said 42526, Egypt

ARTICLE INFO

Article history:
Received 7 July 2025
Received in revised form 18 August 2025
Accepted 25 August 2025
Available online 2 September 2025

Keywords:
Experimental; finite element analysis; composite materials; ANSYS; aerodynamic; wind turbine blade

ABSTRACT

Wind energy is an essential source of sustainable and renewable energy. This paper discussed the strain, stress and deformation procedure involving a small lab-scale wind turbine rotor. In this paper, using a 1.5 MW scale wind turbine as the prototype, the study included selecting an NREL S818-S825-S826 airfoil for General Electric (GE) horizontal axis wind turbine (HAWT) and determining the material properties of composite materials with different layers of glass fibres. The laboratory experiment and the ANSYS program were conducted to perform a structural analysis of the blade at various wind speeds with different composite materials to calculate the strain, stress and deformation values in the laboratory and compare them with the ANSYS. The simulation analysis considered two independent variables: wind speed (5, 10, 12, 15, 17 m/s) and different composite materials (virgin, one, two and three layers from fiberglass). The result is improved blade design for strain, stresses and deformation. The results showed good agreement between the experimental and the ANSYS simulation.

1. Introduction

Renewable energy, especially wind power, is expected to grow significantly to meet rising global energy demands sustainably. This will require scaling up production capabilities for wind turbine components. One of the main challenges in HAWT design is managing the variable and fluctuating wind loads on the turbine. HAWT are widely used for harnessing wind energy due to their efficiency and reliability. However, the dynamic loading conditions experienced by the blades can lead to significant stresses that may affect their structural integrity and overall performance. Traditional approaches to stress analysis often neglect the influence of fluid flow on structural response, limiting the accuracy of the predictions. Arivalagan *et al.,* [1] presented the design, development and optimization of a PLA-based 3D printed micro horizontal axis wind turbine blade. The study aimed to generate 100 watts of power for low-wind-speed applications. Wang *et al.,* [2] Presented a structural optimization model for wind turbine composite blades based on finite element analysis

* *Corresponding author.*
E-mail address: eslam.shamso@eng.psu.edu.eg

https://doi.org/10.37934/sijmr.4.1.1029

and genetic algorithm. The model minimizes the mass of composite blades with multi-criteria constraints and has been applied to the blade structural optimization of ELECTRA 30 kW wind turbine, resulting in a 17.4% reduction in blade mass. The study presents the design of a blade similar in size to a GE 1.5xle turbine and validates the CFD analysis results through experimental readings, aiming to maximize constant power generation from the HAWT [3]. The simulation analysis considers three independent variables: wind speeds, blade position and five composite materials [4]. The results show a good agreement between the numerical simulation and the values of tip velocity, power coefficient and blade deflection. The presented investigates the impact of varying pitch angles and angular velocity on the performance parameters of a HAWT using CFD simulations [5]. The study compared the performance of five composite materials and found that wind speed influenced blade deformation and von Mises stresses [6]. Roul *et al.,* [7] examined the effect of different wind velocities and pitch angles on the performance of the wind turbine, emphasizing the importance of pitch angles. Shamso *et al.,* [8] present a complete analysis of fatigue life within a horizontal axis wind turbine blade HAWT under cyclic loads and variable stresses have been investigated by using the Goodman theory. Belfkira *et al.,* [9] presented a study on optimizing wind turbine blade materials using natural fibres through a hybridization technique. Song *et al.,* [10] Presented an optimization design program for the aerodynamic contour of wind turbine blades using MATLAB. It also proposes a modelling method for the dynamic analysis of composite blades using SolidWorks and ANSYS. The computational fluid dynamics (CFD) analysis of a wind turbine (WT) blade is a crucial aspect that requires careful consideration by designers [11-13]. Shamso *et al.,* [14], presented the stress analysis of wind turbine blades using CFD and FEA simulations, specifically for HAWT. The study utilizes the software ANSYS for modelling complex shapes and simulating FSI. The CFD model calculates aerodynamic loads, while the FEA model determines structural blade responses. Domnica *et al.,* [15] study aims to optimize the design of composite materials used in wind turbine blades with HAWT using FE analysis. The study focuses on the structural optimization of the composite material to improve the performance and efficiency of wind turbines. The turbulence model SST is a popular CFD model for simulating turbulent flows [16-18]. Wang *et al.,* [19] demonstrate a practical method for optimizing the blade design of fixed-pitch fixed-speed wind turbines based on aerodynamic characteristics and design parameters. Zhu *et al.,* [20] propose optimizing wind turbine blade design by considering the static aeroelastic effects between fluid-structure interaction. The method aims to increase annual energy production and reduce blade mass by employing key parameters of the blade as design variables and considering various design requirements as constraints. Shakya *et al.,* [21] focused on Fluid-structure interaction and life prediction of small-scale damaged horizontal axis wind turbine blades. Paulsen *et al.,* [22] presented the optimized blade profile has a low weight and high stiffness. Muskulus *et al.,* [23] Presented the challenges and possible approaches for the structural optimization of wind turbines, focusing on towers, support structures and foundation systems. It highlights the importance of computer-aided approaches in finding better and more economical solutions. Tawade *et al.,* [24] presented how to minimize the cost of wind turbine plants by optimizing the fatigue life of their blades. The authors utilize ANSYS software to analyse the finite element model of the blade and employ Morrow's Equation to determine the blade's fatigue life. Derakhshan *et al.,* [25] presented to study the aerodynamic performance of wind turbine blades and developed an efficient approach for shape optimization of blades using an artificial bee colony algorithm coupled with artificial neural networks. Jureczko *et al.,* [26] presented the optimization of composite wind turbine blades by selecting the optimal material and geometric properties to reduce the costs of making the entire wind turbine. A two-criteria optimization task was formulated to minimize the mass and vertical deflection of the wind turbine blade. Peng *et al.,* [27], presented the Taguchi method for optimization analysis. The study determines the optimal parameter settings for

twin array units to increase power performance. Chen *et al.,* [28] presented a procedure to optimize the composite structures of a 2 MW wind turbine blade using a combination of finite element analysis and particle swarm algorithm. The optimized blades show a reduction in mass compared to the initial blade, which has significant implications for the structural design and optimization of wind turbine blades. Muhsen *et al.,* [29] presented to design and optimize the performance of a small horizontal-axis wind turbine to obtain a power coefficient (CP) higher than 40% at a low wind speed of 5 m/s.

This paper uses experimental analysis and ANSYS finite element analysis to determine stress analysis (structural analysis), material comparison and optimal selection of horizontal axis wind turbines (HAWT). This research aims to use a test to measure strain, stress and deformation under the influence of aerodynamic loading of wind turbine blades. Performance analysis was performed on small-sized wind turbines. To achieve the goal, the performance of wind turbines was measured under different speeds and different composite materials, to measure strain, stress and deformation, compare them and choose the best material under different conditions.

2. Methodology

The study employed a methodology that involved several steps to analyse the structural behaviour of wind turbine blades made from composite materials. Here is a methodology breakdown: airfoil selection, material properties, laboratory experiment and ANSYS analysis. Comparison of experimental and simulation results: The results obtained from the laboratory experiment and the ANSYS simulation were compared to evaluate the agreement between the two.

3. Wind Turbine Rotor Models

3.1 Blade CAD Model

The ANSYS design modeler was used to create the 3D CAD model of the blade [11,13,30,31]. Each airfoil is sketched using its coordinates and then scaled to the chord length. The airfoils are then bent throughout the blade span. Finally, the airfoils were lofted to create the blade surface [16,30]. Table 1 and Figure 1 display each cross-section's location, chord length and twist angle from the Sandia reference study [3,7,31,32].

Table 1
Rotor specifications

Parameters	Values	Units
Airfoil (NREL)	S818-S825-S826	-
Rotor radius	0.2	m
Free stream velocity (Vw)	5-10-12-15	m/s
Air density	1.225	kg/m^3

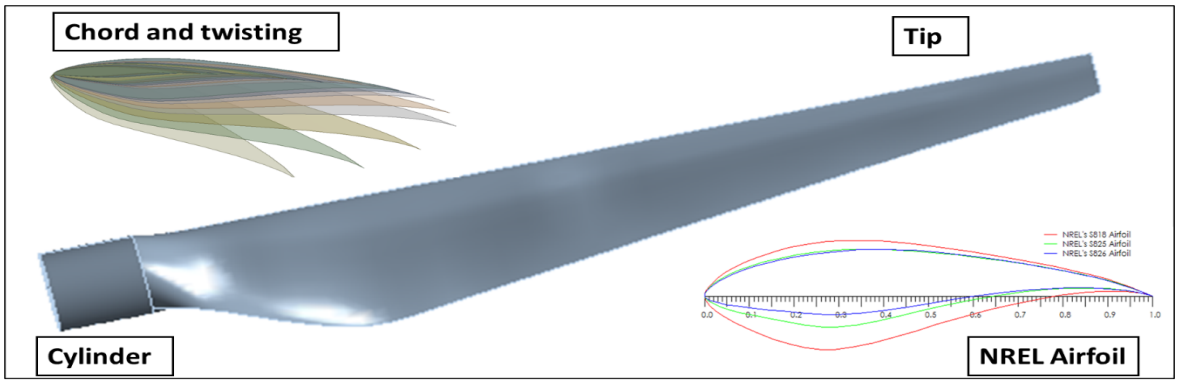

Fig. 1. Blade CAD model

3.2 Model of a Wind Turbine Blade

The turbine model utilized in this study features three cross-section twisted blades, each with a length of 20 cm. The profile shape of the blades was based on the commonly used NREL 818,825 and 826 airfoil series. Polylactic acid (PLA) material was used to manufacture the blade and a 3D printer was employed to create the first product. The blades are produced from fiberglass material by moulding and are employed to produce the final product, as illustrated in Figure 2.

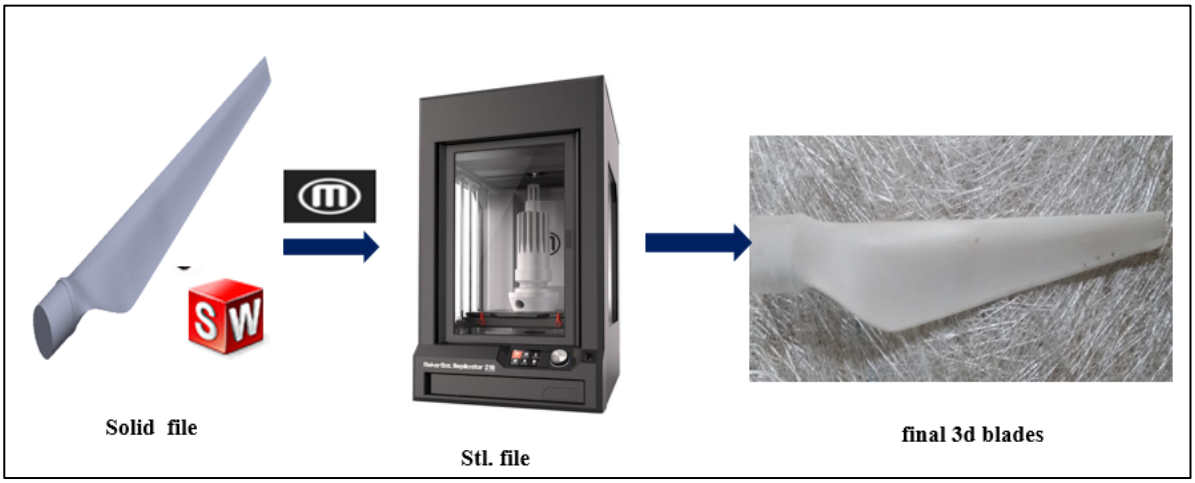

Fig. 2. Blade made of PLA

3.3 The Blade is Made of Fiberglass (Composite Materials)

Figure 3 shows the different methods for manufacturing wind turbine blades on a large and small scale, such as 3D printing, moulds and machining. On the other hand, on a small scale, machining processes such as CNC are used for their accuracy and obtaining the highest surface roughness quality, but their cost is high compared to other methods. The second method, manufacturing using 3D printing, is used in small-scale turbine blades due to the ease of the manufacturing process for complex shapes and the low cost, but it is not strong compared to other methods. The third method used in the large dimensions of wind turbine blades is making a mould. From here, an idea was created, which is how to make a turbine blade with small dimensions that has high quality and strength by manufacturing a mould of fiberglass and silicone to manufacture the turbine blade and controlling the number of layers of fiberglass inside the blade, so to strengthen it, considering the low cost of manufacturing and obtaining a template product for implementation in industry.

Building a mould for a wind turbine involves several steps. Here are the general steps involved in constructing the mould: Design and Blueprint: Begin by designing the wind turbine blade using computer-aided design (CAD) SolidWorks software. Determine the blade dimensions, shape and specific requirements for this paper. Construct a detailed blueprint with all the necessary features and measurements, as shown in Figure 3 and Figure 4. It's important to note that building a mould for a wind turbine blade made of fiberglass is a complex process that requires expertise in composite manufacturing techniques.

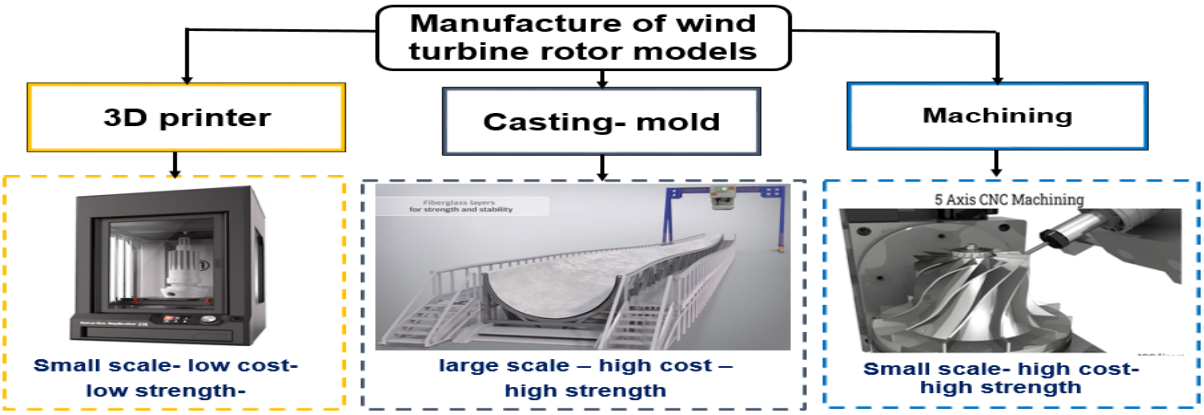

Fig. 3. Flow chart of manufacture of wind turbine rotor blade

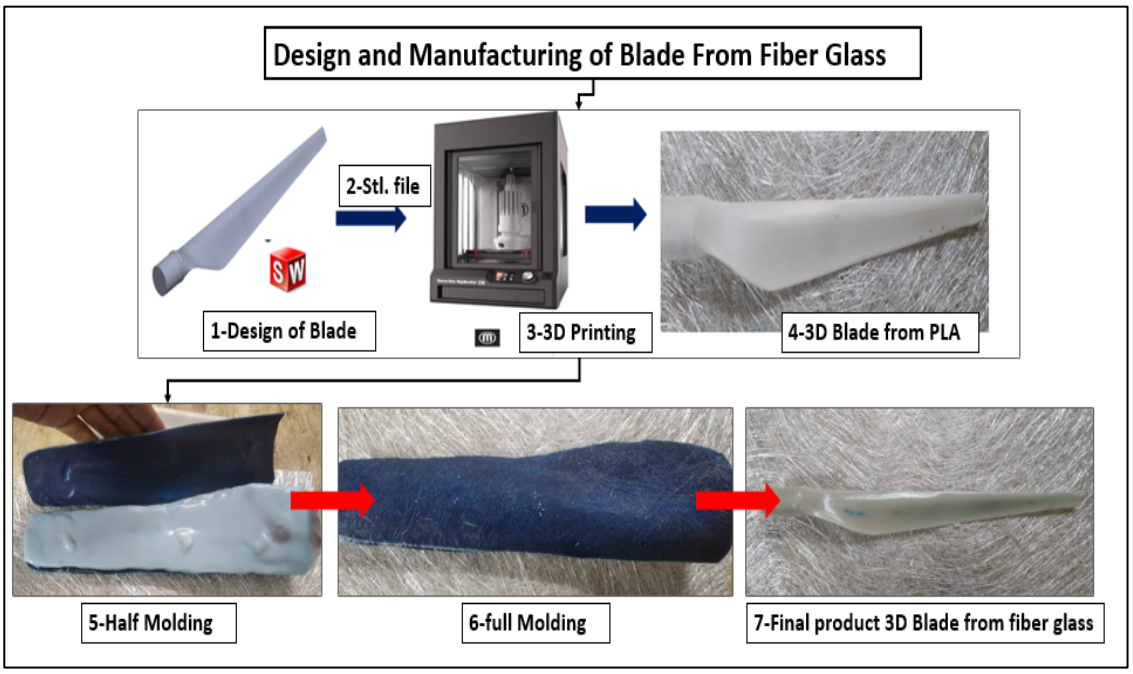

Fig. 4. Final blade from fiberglass

4. Experimental Setup and Procedure

4.1 Wind Tunnel (External) and Specifications of Wind Tunnel Compartment

This experiment measures various readings of a wind turbine model's output strain, stress and deformation with varying wind speeds. The wind tunnel is a well-known experimental setup for conducting aerodynamic flow experiments. The wind tunnel used in this study is of the low-speed blower type with an open-jet design and it consists of two branches; each supplied with air from two centrifugal blowers. These blowers have a power of 5.5 kW each and are connected to the tunnel

leg through flexible joints to reduce vibration. The airflow rate through the tunnel is regulated by an AC inverter made by Toshiba (model VF-S11), which controls the rotational speed of the blowers by connecting their motors in parallel to the inverter circuit. The nozzle exits cross-section has a 60 × 60 cm dimension, as illustrated in Figure 5.

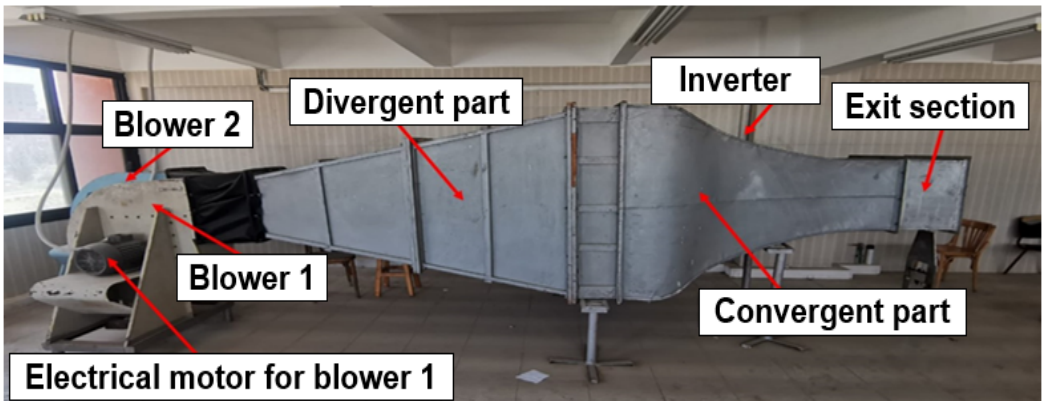

Fig. 5. The wind tunnel of the mechanical power engineering department in Port Said

4.2 Experimental Procedure - Wind Turbine Model- Single-Blade Test

The wind turbine model comprises three main parts: the blade, the steel stand and the strain gauge, as shown in Figure 6. Scales were made suitable for the turbine blade size, from 41.25 m to 0.2 m in length. The model of the turbine has the following specifications: A blade with three different national renewable energy laboratories (NREL) (S818, S825, S826), respectively and a 130 cm height frame, which is mounted to fix the turbine rotor with frame and a steel frame is used to fix the turbine. The turbine rotor is placed at the centre in front of the duct exit, as shown in Figure 6. The technical specifications of the wind turbine rotor are listed in Table 1. The wind tunnel tests focused on studying the aerodynamic forces acting on the blade. The blades were mounted vertically on a support strut aligned with the flow direction. The strut was connected to a strain gauge on the wind blade. This experiment was conducted for all four blade design configurations using various composite materials. Figure 6 illustrates the experimental arrangement of the blade in the wind tunnel test section.

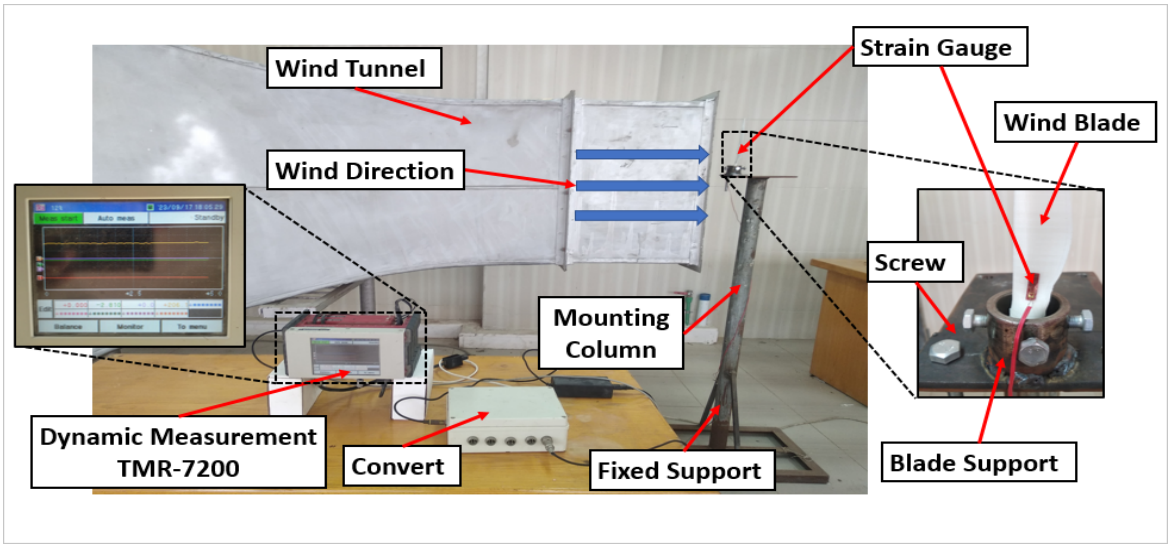

Fig. 6. The test rig of a single blade is mounted vertically in the wind tunnel

4.3 Wind Turbine Blade FE Model

The wind turbine blade was created using SolidWorks software, then scaled and printed using a 3D printer. The wind turbine blade was designed using Solidworks software and scaled to the desired size. A 3D printer produced a physical prototype of the blade to bring the design into reality. This study chose a 1.5 MW renewable energy horizontal axis wind turbine (HAWT) manufactured by GE as a case study. Figure 1 and Table 1 provide the necessary information regarding this turbine as a reference for the study's analysis and evaluation.

4.4 Material Properties

Composite materials are crucial in manufacturing horizontal and vertical wind turbine blades. In this study, wind turbine blades were 3D printed and cast using different composite materials. The dimensions of the specimens were based on the ASTM D638 standard for tensile properties of plastics, as illustrated in Figure 7. A 3D model of the specimen was created using computer-aided software such as SolidWorks and saved in the standard tessellation language (.STL) file format for printing and casing, as shown in Figure 7.

The properties of the blade, including Young's modulus and Poisson's ratio, for each material were obtained by varying the layers' value (Lf) at virgin (zero), one, two and three layers using the appropriate tool. These properties are presented in Table 2. Where E is Young's modulus, υ is Poisson's ratio. The specific materials used in the experimental and ANSYS.

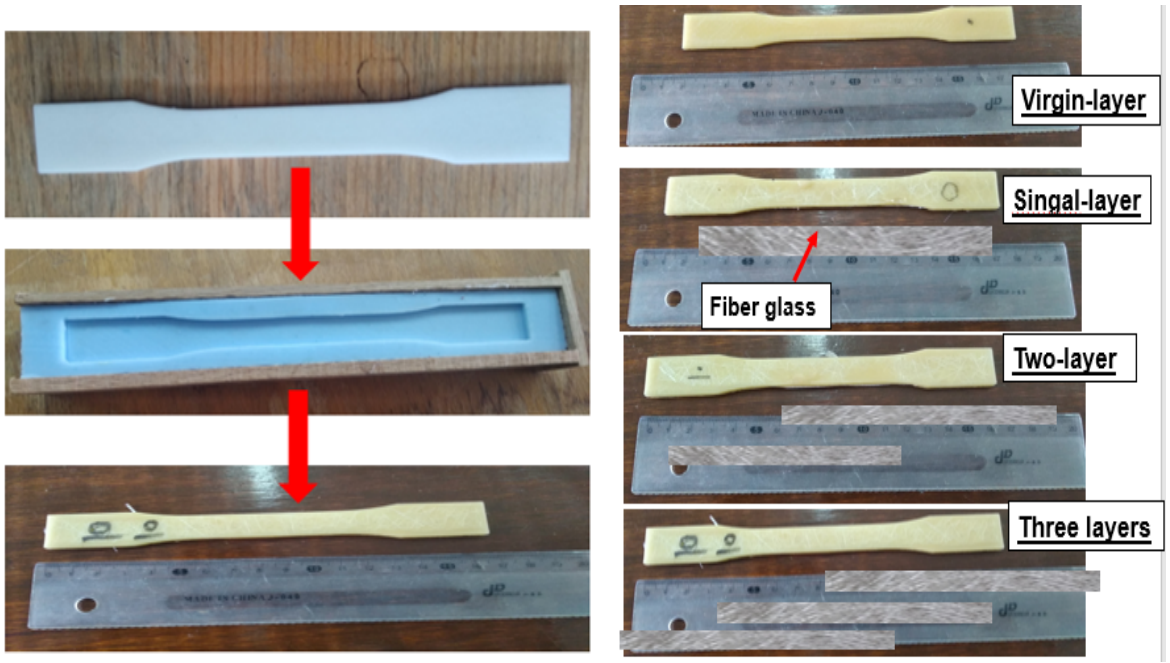

Fig. 7. Composite material specimens using the mould

Table 2
Material properties of fiberglass (composite material)

Material layers	Fiber Virgin (zero)	Fiber layers one	Fiber two	Fiber three
E (GPa)	1.6	3.3	4.1	6.6
υ	0.3	0.3	0.3	0.3

4.5 FEA Mesh

Figure 8 shows the (HAWT) with a blade length of 20 cm. A mesh was created for the turbine blade to conduct further analysis. The meshing process involved utilizing a tetrahedral mesh element mesh size of 2 mm. This meshing approach enabled the division of the blade into 47,915 nodes and 26,128 elements. The following element sizes are investigated at blade surfaces: 5 mm, 4 mm, 3 mm, 2 mm and 1 mm.

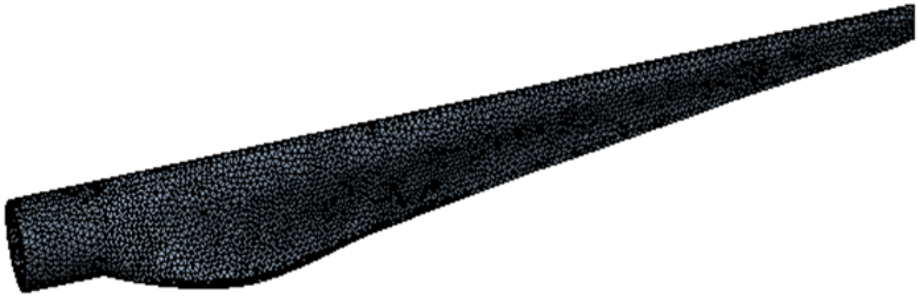

Fig. 8. FEA mesh blade

Figure 9 and Table 3 show the number of elements and the deformation converges at an element size of 2 mm. Further refinement of the element size significantly increases the computational time; an element size of 2 mm is estimated in this study.

Table 3
Mesh independency study

Item	Mesh independency study				
Mesh el. size (mm)	5	4	3	2	1
Deformation (mm)	0.69397	0.69886	0.70237	0.70482	0.70551
No. of Elements	2187	3129	5719	26128	126265

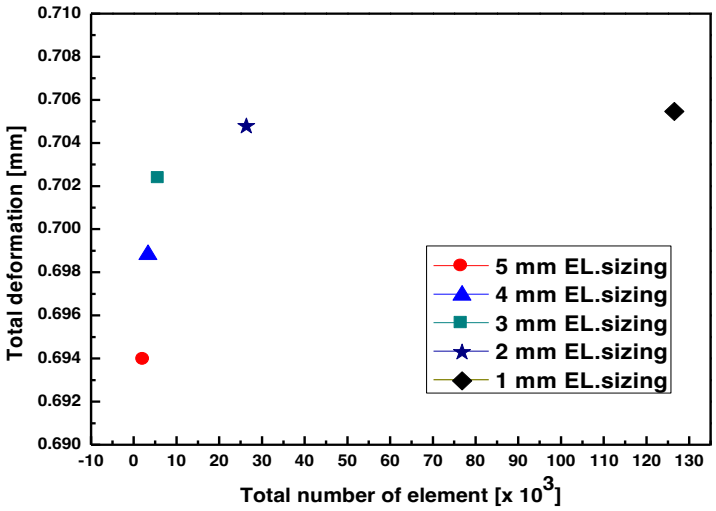

Fig. 9. Mesh independency study

4.6 Boundary Conditions of Blade

A finite element method is employed in the structural workbench of ANSYS to generate the structural model of the blade. This study examined a structural analysis component in the ANSYS workbench. Figure 10 shows the schematic of the modelling (boundary conditions of the blade). The boundary of FEA modelling can be done after defining the blade geometry, material properties, mesh, boundary conditions and different types of structural analysis. The HAWT is fixed while fully constrained in all directions at the fixed end to prevent rigid body motion and the blade is assumed to be a cantilever beam attached to a rotating ring see Figure 10.

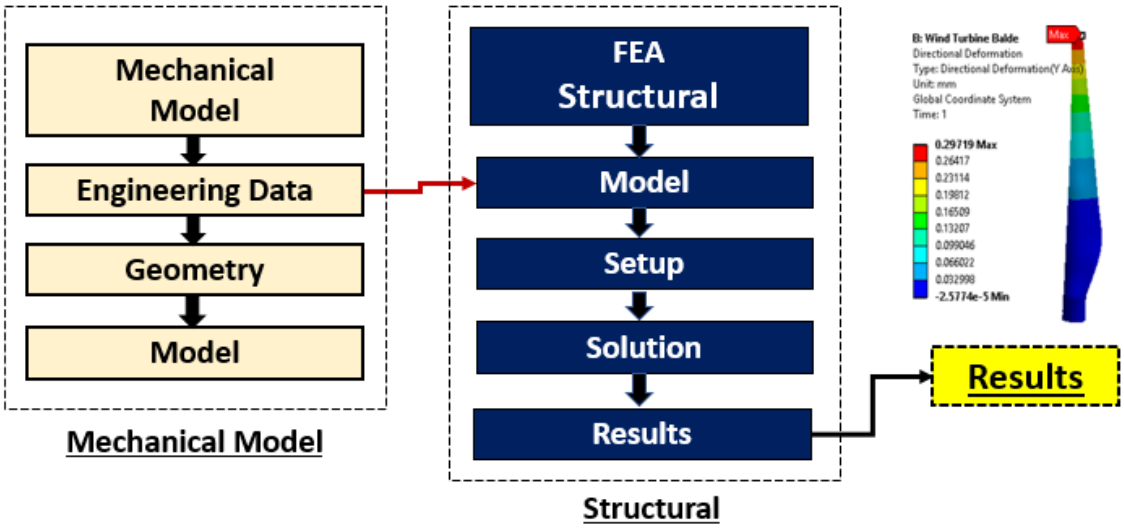

Fig. 10. Schematic of modelling (boundary conditions of the blade)

5. Results and Discussions

5.1 Experimental Work Results

In this section, the results obtained from laboratory experiments and numerical analysis are extracted and compared, such as the values of strain, stress, strain energy and max deformation, as illustrated in Table 4, Figure 11, Figure 12, Figure 13 and Figure 14.

5.2 Strain for Blade

The graph illustrates the relationship between wind speed and strain values using two different methods: parametric experiment and finite element analysis (FEA) with the ANSYS program, as shown in Figure 11. The study focuses on composite materials such as PLA. The wind speed range considered in the experiment and ANSYS simulations was from 5 to 20 m/s. In the parametric experiment, the strain value increased as the wind speed increased. For instance, at a wind velocity of 5 m/s, the strain reached 1.78×10^{-5}. It further increased to 9.1×10^{-5} at a velocity of 10 m/s. At a wind velocity of 15 m/s, the strain reached 20.3×10^{-5}.

On the other hand, in the ANSYS simulations, the strain values also showed an increasing trend with increasing wind speed. At a velocity of 5 m/s, the strain was 2.28×10-5. At a velocity of 10 m/s, the strain was 8.31×10^{-5} and it further increased to 18.36×10^{-5} at a velocity of 17 m/s. These results show that both the parametric experiment and ANSYS simulations show a positive correlation between wind speed and strain values in composite materials like PLA. Higher wind speeds lead to

higher strain values, suggesting increased deformation and stress on the material. These findings can supply valuable insights for designing composite wind turbine blades and assessing their structural performance under varying wind conditions.

Table 4
Results values using two different methods: experiment and (FEA)

Parameters	unit	Wind velocity (m/s)					
Wind Velocity	(m/s)	5	7	10	12	15	17
Experimental Strain×10^{-5}	-	1.78	-	9.1	-	20.3	-
ANSYS Strain×10^{-5}	-	2.28	4.21	8.31	11.85	18.36	23.35
Experimental Stress (Hook law) 10^{5}	Pa	0.55	-	2.82	-	6.29	-
ANSYS Stress ×10^{5}	Pa	0.56	1.33	2.63	3.75	5.82	7.45
ANSYS Deformation	mm	0.077	0.147	0.297	0.426	0.66	0.851
Strain Energy×10^{-7}	J	0.118	0.386	1.469	2.96	7.06	11.55

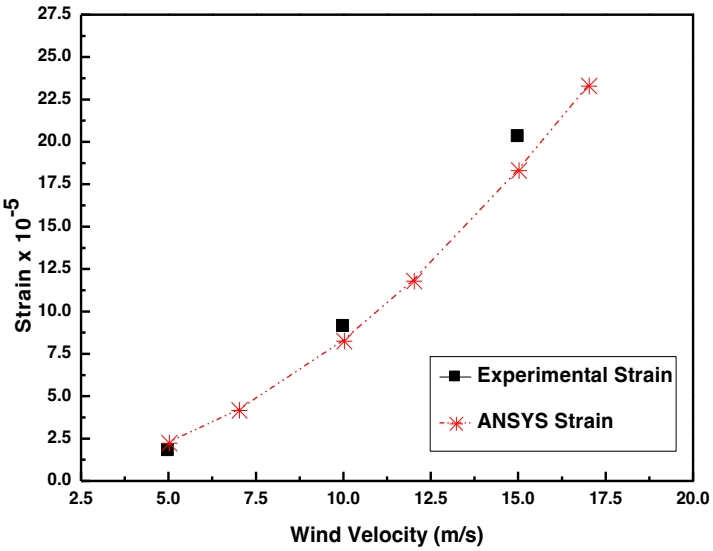

Fig. 11. Strain values using two different methods: experiment and (FEA)

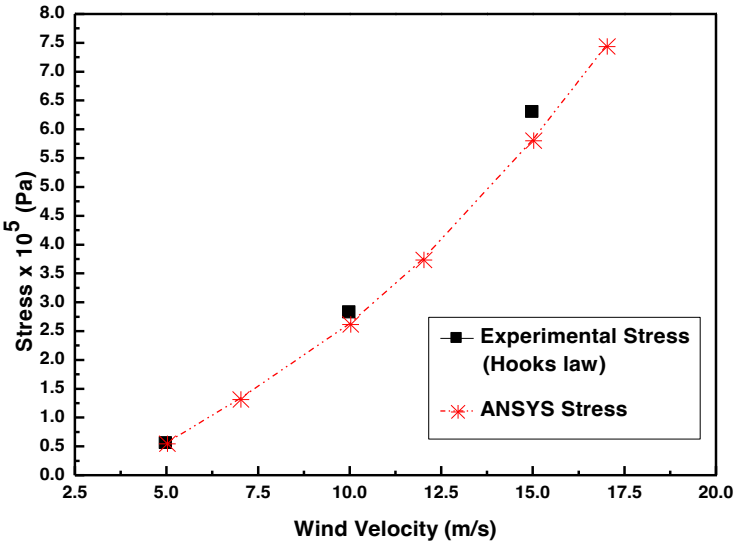

Fig. 12. Stress values using two different methods: Experiment and (FEA)

5.3 Deflections for Blade

The graph illustrates the relationship between wind speed and deformation values, an increasing trend in deformation for composite materials, specifically PLA, as wind velocities range from 5 to 20 m/s. At a wind velocity of 5 m/s, the deformation reaches 0.077 mm and further increases to 0.147 mm at a velocity of 7 m/s. The deformation continues to rise, reaching 0.297 mm at a velocity of 10 m/s. Subsequently, at a wind velocity of 15 m/s, the deformation increases to 0.66 mm and it further escalates to 0.851 mm at a velocity of 17 m/s. These findings suggest that as wind velocities increase, the deformation of the composite material, specifically PLA, also increases. The increasing deformation shows the blade's response to the applied wind loads, as shown in Figure 13, with higher wind velocities resulting in more significant deformations. Considering these deformation values in the design and analysis of wind turbine blades is essential to ensure their structural integrity under varying wind conditions.

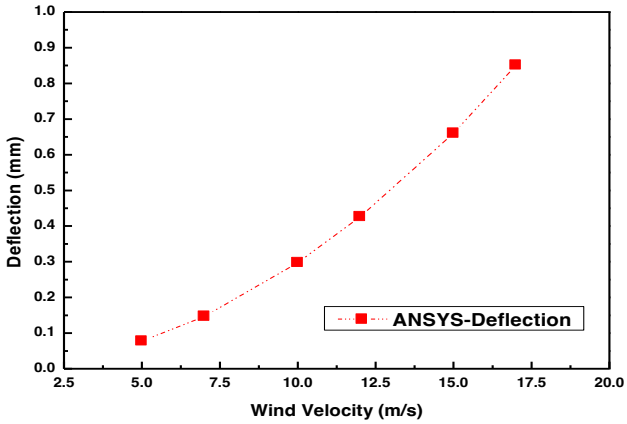

Fig. 13. Deformation results of PLA using ANSYS

Figure 14 shows the relationship between deformation and different wind speeds, ranging from 5 to 17 m/s and the comparison between other composite materials and PLA. At low speeds, the deformation values were similar between the different materials. When wind speeds increase, the deformation values increase. With virgin material, we find that the deformation values are extensive

and at different speeds than those of other materials. On the other hand, materials with glass fibres have more strength and less deformation compared to PLA.

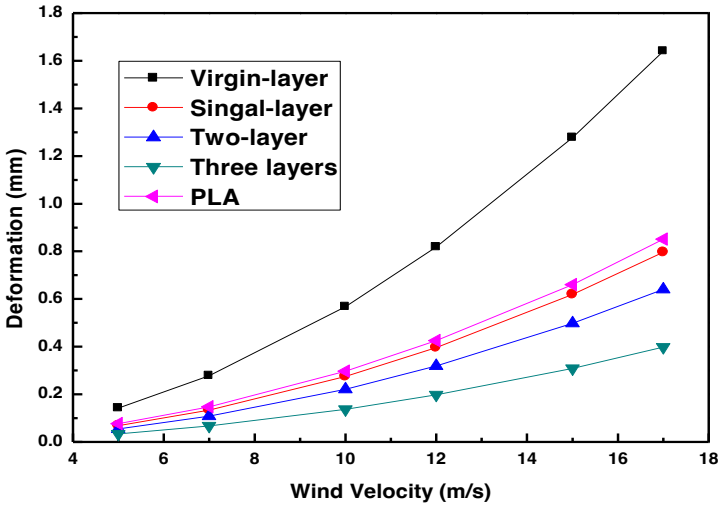

Fig. 14. Deformation values and wind velocity for different composite materials using ANSYS

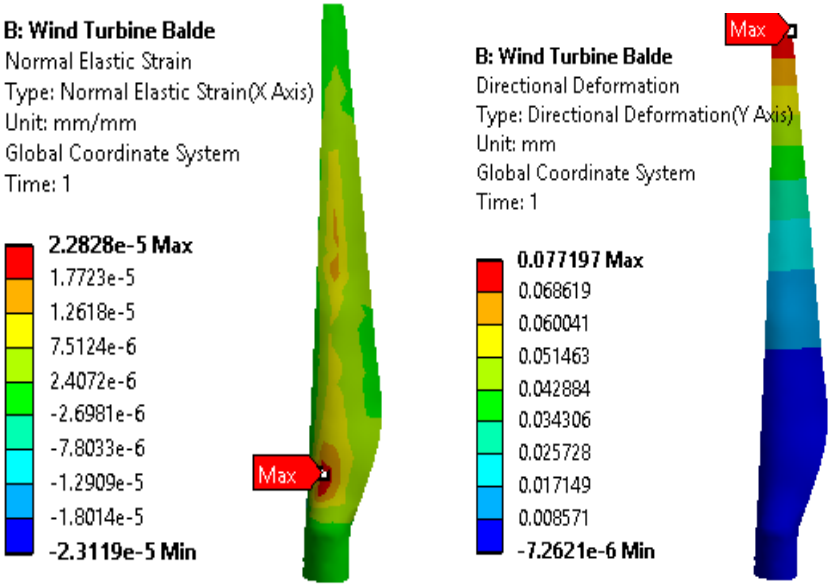

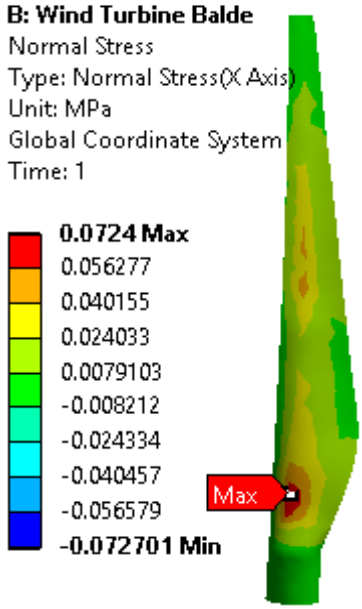
B: Wind Turbine Balde
Normal Stress
Type: Normal Stress(X Axis)
Unit: MPa
Global Coordinate System
Time: 1
0.0724 Max
0.056277
0.040155
0.024033
0.0079103
-0.008212
-0.024334
-0.040457
-0.056579
-0.072701 Min
Max

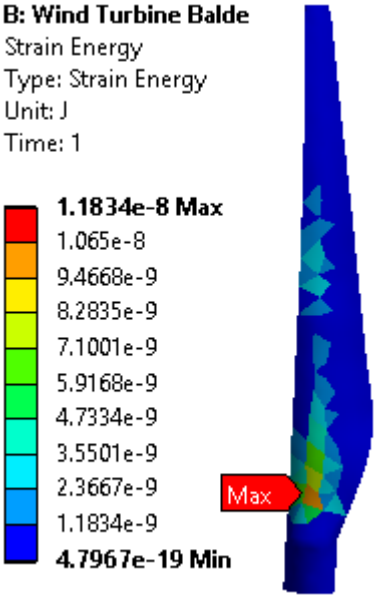
B: Wind Turbine Balde
Strain Energy
Type: Strain Energy
Unit: J
Time: 1
1.1834e-8 Max
1.065e-8
9.4668e-9
8.2835e-9
7.1001e-9
5.9168e-9
4.7334e-9
3.5501e-9
2.3667e-9
1.1834e-9
4.7967e-19 Min
Max

At V= 5 m/s

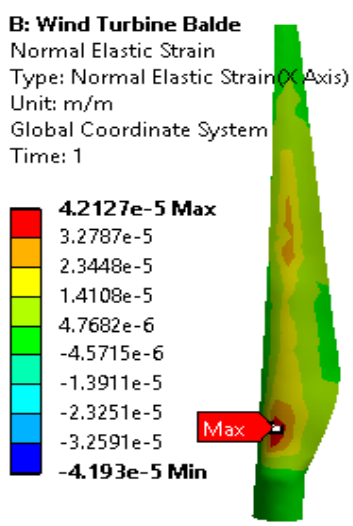
B: Wind Turbine Balde
Normal Elastic Strain
Type: Normal Elastic Strain(X Axis)
Unit: m/m
Global Coordinate System
Time: 1
4.2127e-5 Max
3.2787e-5
2.3448e-5
1.4108e-5
4.7682e-6
-4.5715e-6
-1.3911e-5
-2.3251e-5
-3.2591e-5
-4.193e-5 Min
Max

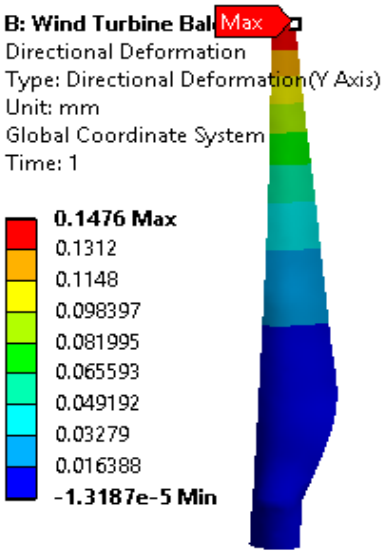
B: Wind Turbine Bal
Max
Directional Deformation
Type: Directional Deformation(Y Axis)
Unit: mm
Global Coordinate System
Time: 1
0.1476 Max
0.1312
0.1148
0.098397
0.081995
0.065593
0.049192
0.03279
0.016388
-1.3187e-5 Min

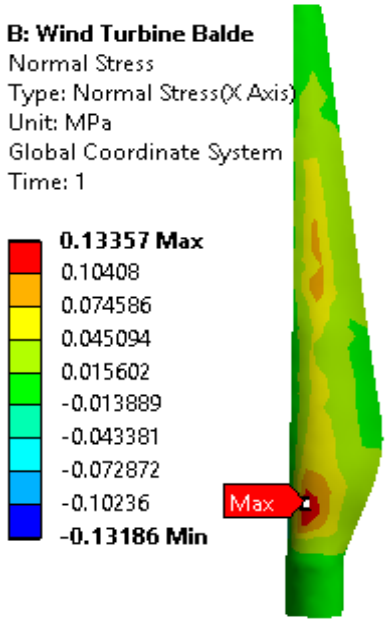
B: Wind Turbine Balde
Normal Stress
Type: Normal Stress(X Axis)
Unit: MPa
Global Coordinate System
Time: 1
0.13357 Max
0.10408
0.074586
0.045094
0.015602
-0.013889
-0.043381
-0.072872
-0.10236
-0.13186 Min
Max

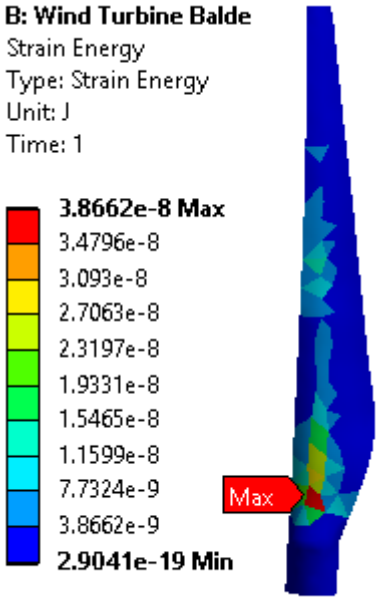
B: Wind Turbine Balde
Strain Energy
Type: Strain Energy
Unit: J
Time: 1
3.8662e-8 Max
3.4796e-8
3.093e-8
2.7063e-8
2.3197e-8
1.9331e-8
1.5465e-8
1.1599e-8
7.7324e-9
3.8662e-9
2.9041e-19 Min
Max

At V= 7 m/s

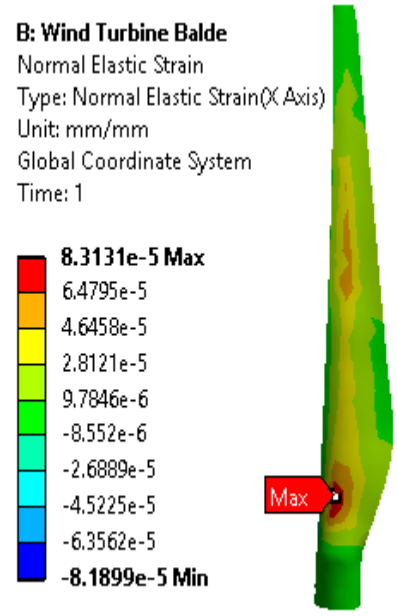
B: Wind Turbine Balde
Normal Elastic Strain
Type: Normal Elastic Strain(X Axis)
Unit: mm/mm
Global Coordinate System
Time: 1
8.3131e-5 Max
6.4795e-5
4.6458e-5
2.8121e-5
9.7846e-6
-8.552e-6
-2.6889e-5
-4.5225e-5
-6.3562e-5
-8.1899e-5 Min
Max

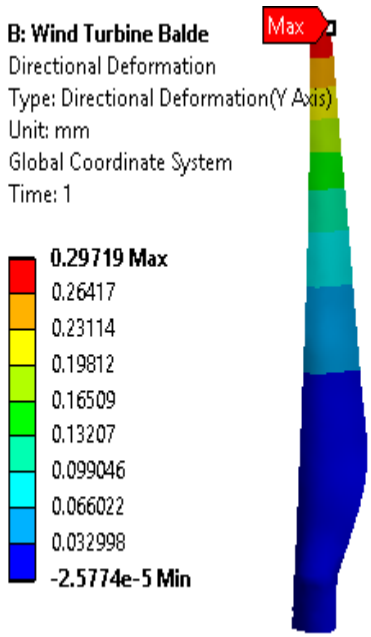
B: Wind Turbine Balde
Directional Deformation
Type: Directional Deformation(Y Axis)
Unit: mm
Global Coordinate System
Time: 1
0.29719 Max
0.26417
0.23114
0.19812
0.16509
0.13207
0.099046
0.066022
0.032998
-2.5774e-5 Min
Max

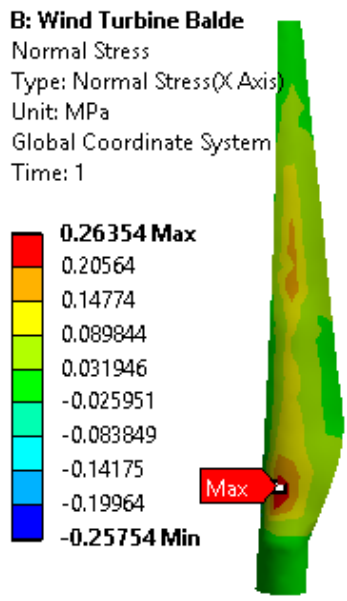
B: Wind Turbine Balde
Normal Stress
Type: Normal Stress(X Axis)
Unit: MPa
Global Coordinate System
Time: 1
0.26354 Max
0.20564
0.14774
0.089844
0.031946
-0.025951
-0.083849
-0.14175
-0.19964
-0.25754 Min
Max

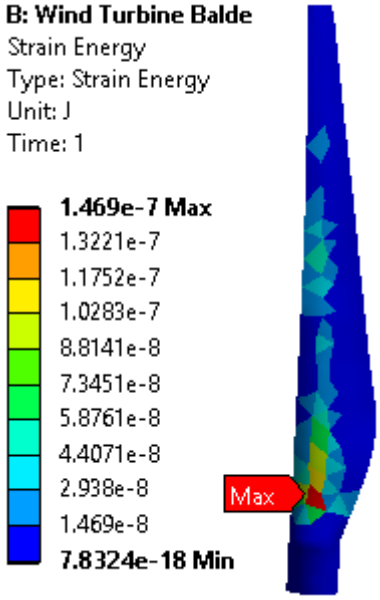
B: Wind Turbine Balde
Strain Energy
Type: Strain Energy
Unit: J
Time: 1
1.469e-7 Max
1.3221e-7
1.1752e-7
1.0283e-7
8.8141e-8
7.3451e-8
5.8761e-8
4.4071e-8
2.938e-8
1.469e-8
7.8324e-18 Min
Max

At V =10 m/s

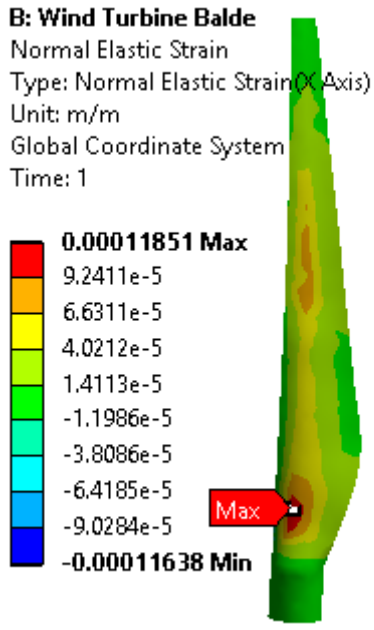
B: Wind Turbine Balde
Normal Elastic Strain
Type: Normal Elastic Strain(X Axis)
Unit: m/m
Global Coordinate System
Time: 1
0.00011851 Max
9.2411e-5
6.6311e-5
4.0212e-5
1.4113e-5
-1.1986e-5
-3.8086e-5
-6.4185e-5
-9.0284e-5
-0.00011638 Min
Max

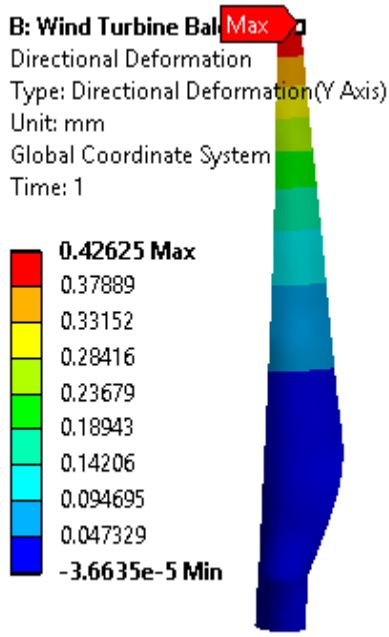
B: Wind Turbine Bal
Directional Deformation
Type: Directional Deformation(Y Axis)
Unit: mm
Global Coordinate System
Time: 1
0.42625 Max
0.37889
0.33152
0.28416
0.23679
0.18943
0.14206
0.094695
0.047329
-3.6635e-5 Min
Max

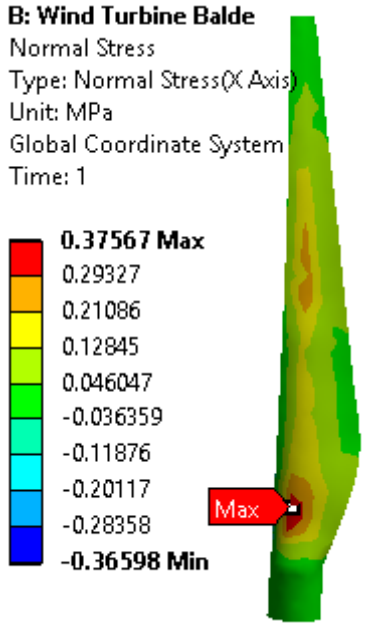
B: Wind Turbine Balde
Normal Stress
Type: Normal Stress(X Axis)
Unit: MPa
Global Coordinate System
Time: 1
0.37567 Max
0.29327
0.21086
0.12845
0.046047
-0.036359
-0.11876
-0.20117
-0.28358
-0.36598 Min
Max

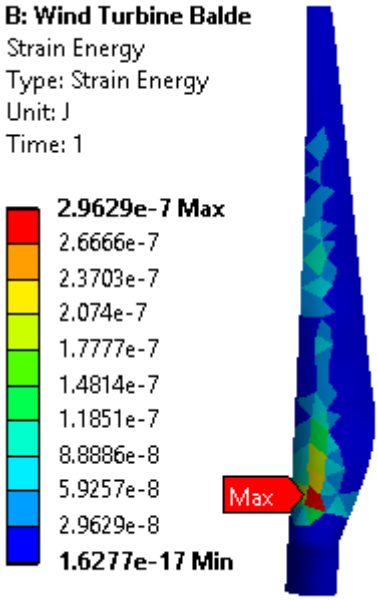
B: Wind Turbine Balde
Strain Energy
Type: Strain Energy
Unit: J
Time: 1
2.9629e-7 Max
2.6666e-7
2.3703e-7
2.074e-7
1.7777e-7
1.4814e-7
1.1851e-7
8.8886e-8
5.9257e-8
2.9629e-8
1.6277e-17 Min
Max

V= 12 m/s

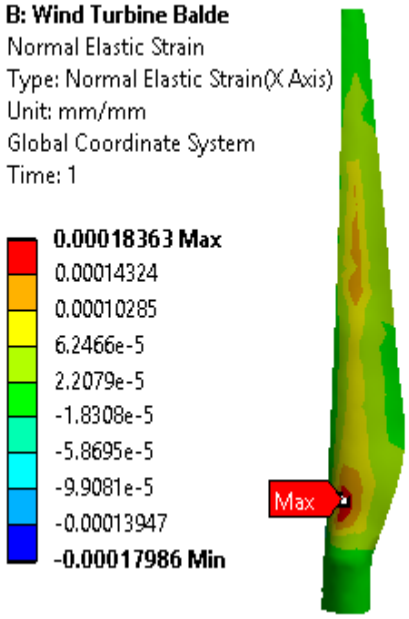
B: Wind Turbine Balde
Normal Elastic Strain
Type: Normal Elastic Strain(X Axis)
Unit: mm/mm
Global Coordinate System
Time: 1
0.00018363 Max
0.00014324
0.00010285
6.2466e-5
2.2079e-5
-1.8308e-5
-5.8695e-5
-9.9081e-5
-0.00013947
-0.00017986 Min
Max

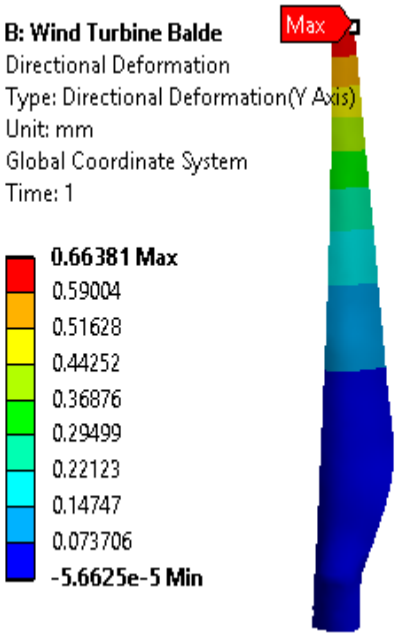
Max
B: Wind Turbine Balde
Directional Deformation
Type: Directional Deformation(Y Axis)
Unit: mm
Global Coordinate System
Time: 1
0.66381 Max
0.59004
0.51628
0.44252
0.36876
0.29499
0.22123
0.14747
0.073706
-5.6625e-5 Min

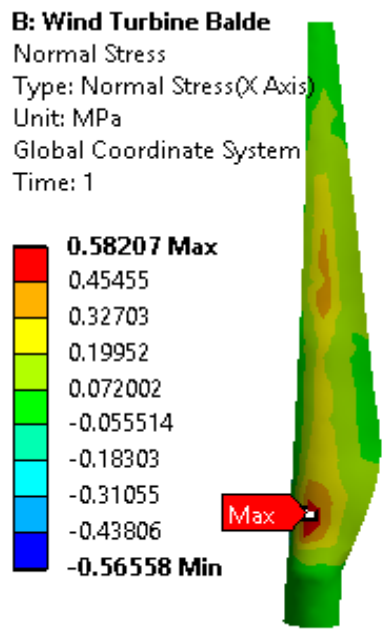
B: Wind Turbine Balde
Normal Stress
Type: Normal Stress(X Axis)
Unit: MPa
Global Coordinate System
Time: 1
0.58207 Max
0.45455
0.32703
0.19952
0.072002
-0.055514
-0.18303
-0.31055
-0.43806
-0.56558 Min
Max

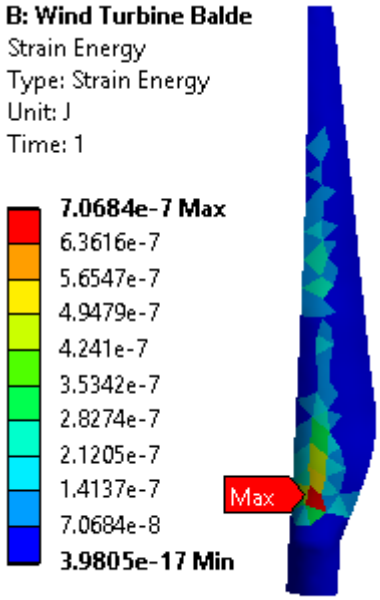
B: Wind Turbine Balde
Strain Energy
Type: Strain Energy
Unit: J
Time: 1
7.0684e-7 Max
6.3616e-7
5.6547e-7
4.9479e-7
4.241e-7
3.5342e-7
2.8274e-7
2.1205e-7
1.4137e-7
7.0684e-8
3.9805e-17 Min
Max

At V =15 m/s

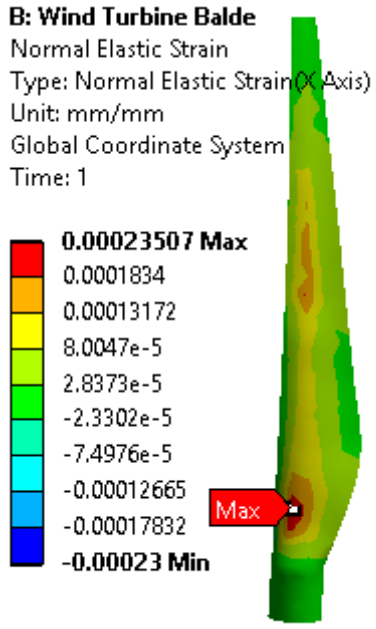
B: Wind Turbine Balde
Normal Elastic Strain
Type: Normal Elastic Strain(X Axis)
Unit: mm/mm
Global Coordinate System
Time: 1
0.00023507 Max
0.0001834
0.00013172
8.0047e-5
2.8373e-5
-2.3302e-5
-7.4976e-5
-0.00012665
-0.00017832
-0.00023 Min
Max

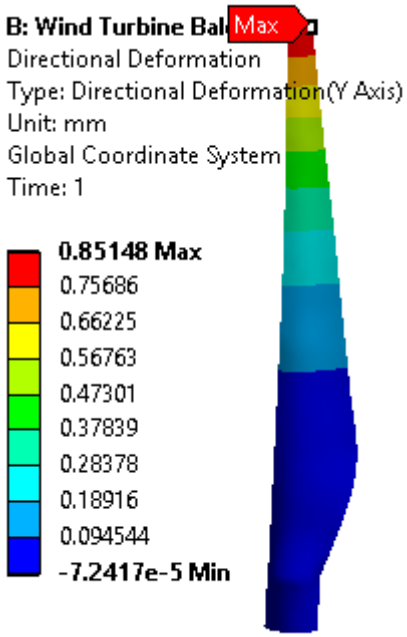
B: Wind Turbine Bal
Max
Directional Deformation
Type: Directional Deformation(Y Axis)
Unit: mm
Global Coordinate System
Time: 1
0.85148 Max
0.75686
0.66225
0.56763
0.47301
0.37839
0.28378
0.18916
0.094544
-7.2417e-5 Min

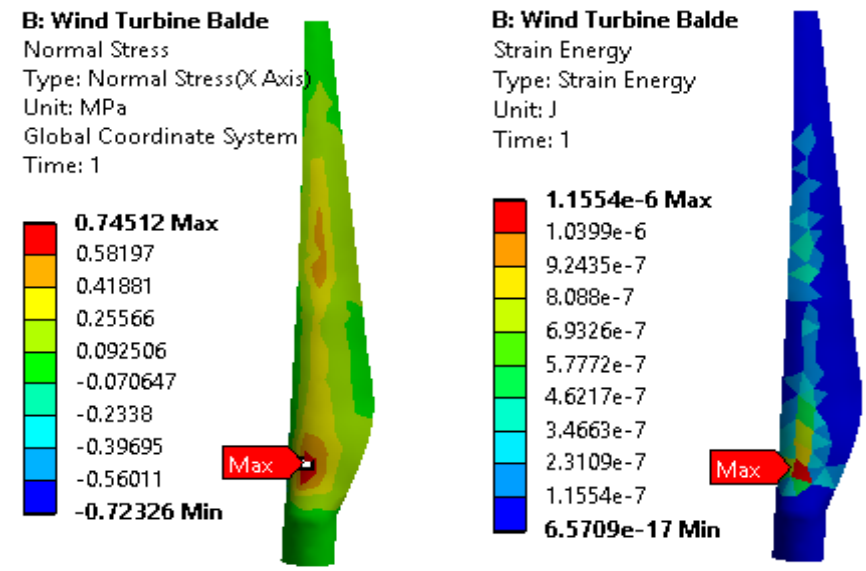

V= 17 m/s

Fig. 15. The strain, stress and deformation values with different wind velocity using (FEA)

6. Conclusion

This simulation shows the workflow of creating a complex shape using ANSYS analysis. Set up simplified finite elements for wind turbine blades. The study described focuses on using composite materials in wind turbine blades. The specific composite material being investigated includes different layers of fiberglass (virgin, one, two and three layers). The NACA airfoil S818-S825-S826 GE HAWT is the basis for the blade design. The following conclusions can be drawn from the current study:

i. 3D printing technology is used to manufacture complex shapes such as turbine blades.
ii. Manufacturing the turbine blade from composite materials at the lowest cost
iii. The laboratory experiment results and the ANSYS stress, strain and deformation program were very good.
iv. Comparing the results showed that composite materials (fiberglass) are better and stronger than PLA.

The weight of the materials used in wind turbine blades can affect their overall performance. However, this study determined that the weight comparison between fiberglass and PLA materials was negligible regarding its influence on the power coefficient.

Acknowledgement
This research was not funded by any grant.

References

[1] Arivalagan, Suresh, Rajakumar Sappani, Robert Čep and Mahalingam Siva Kumar. "Optimization and experimental investigation of 3D printed micro wind turbine blade made of PLA material." *Materials* 16, no. 6 (2023): 2508. https://doi.org/10.3390/ma16062508

[2] Wang, Lin, Athanasios Kolios, Takafumi Nishino, Pierre-Luc Delafin and Theodore Bird. "Structural optimisation of vertical-axis wind turbine composite blades based on finite element analysis and genetic algorithm." *Composite Structures* 153 (2016): 123-138. https://doi.org/10.1016/j.compstruct.2016.06.003
[3] Mezaal, Naji Abdullah, K. V. Osintsev and S. V. Alyukov. "The computational fluid dynamics performance analysis of horizontal axis wind turbine." *International Journal of Power Electronics and Drive Systems* 10, no. 2 (2019): 1072-1080. https://doi.org/10.11591/ijpeds.v10.i2.pp1072-1080
[4] Shamso, Eslam Mohamed, Abla El-Megharbel, Samar Elsanabary, Rasha Soliman and Medhat Awad Elhadek. "Modeling and Response of Horizontal Axis Wind Turbine Blade Based on Fluid-Structure Interaction." *Port-Said Engineering Research Journal* 27, no. 4 (2023): 102-115.
[5] Roul, Rajendra and Awadhesh Kumar. "Effect of different pitch angles on the performance parameter of the horizontal axis wind turbine using computational fluid dynamics." *Authorea Preprints* (2020).
[6] Shamso, Eslam, Medhat El-Hadek, Samar Elsanabary, Abla El-Megharbel and Rasha Soliman. "Finite Element Analysis for Dynamic Simulation of Composite HAWT Blade." *International Journal of Renewable Energy Research (IJRER)* 13, no. 2 (2023): 790-801.
[7] Roul, Rajendra and Awadhesh Kumar. "Fluid-structure interaction of wind turbine blade using four different materials: numerical investigation." *Symmetry* 12, no. 9 (2020): 1467. https://doi.org/10.3390/sym12091467
[8] Shamso, E., M. Elhadek, G. Osmun and A. El-Megharbel. "Fatigue Cycling of NACA 821 Blades in Horizontal Wind Turbines." *SYLWAN* (2019): 79-99.
[9] Belfkira, Z., H. Mounir and A. El Marjani. "Structural optimization of a horizontal axis wind turbine blade made from new hybrid composites with kenaf fibers." *Composite Structures* 260 (2021): 113252. https://doi.org/10.1016/j.compstruct.2020.113252
[10] Song, Fangfang, Yihua Ni and Zhiqiang Tan. "Optimization design, modeling and dynamic analysis for composite wind turbine blade." *Procedia Engineering* 16 (2011): 369-375. https://doi.org/10.1016/j.proeng.2011.08.1097
[11] Resor, Brian Ray and Joshua A. Paquette. *A NuMAD model of the Sandia TX-100 blade*. No. SAND2012-9274. Sandia National Laboratories (SNL), Albuquerque, NM and Livermore, CA (United States), 2012. https://doi.org/10.2172/1055893
[12] Hand, M. Maureen, D. A. Simms, L. J. Fingersh, D. W. Jager, J. R. Cotrell, S. Schreck and S. M. Larwood. *Unsteady aerodynamics experiment phase VI: wind tunnel test configurations and available data campaigns*. No. NREL/TP-500-29955. National Renewable Energy Lab.(NREL), Golden, CO (United States), 2001. https://doi.org/10.2172/15000240
[13] Fluent Ansys, "Ansys Fluent 16.0 Theory Guide." (2016).
[14] Shamso E. and El-Megharbel, A.. "Stress Analysis of Composite Materials in Wind Turbine Blades Subjected to CFD and FEA," *SYLWAN*, no. 163(4), (2019): 330–345.
[15] Domnica, Stanciu Mariana, Curtu Ioan and Tesula Ionut. "Structural optimization of composite from wind turbine blades with horizontal axis using finite element analysis." *Procedia technology* 22 (2016): 726-733. https://doi.org/10.1016/j.protcy.2016.01.031
[16] Lee, Kyoungsoo, Ziaul Huque, Raghava Kommalapati and Sang-Eul Han. "Fluid-structure interaction analysis of NREL phase VI wind turbine: Aerodynamic force evaluation and structural analysis using FSI analysis." *Renewable Energy* 113 (2017): 512-531. https://doi.org/10.1016/j.renene.2017.02.071
[17] Ingram, Grant. "Wind turbine blade analysis using the blade element momentum method. version 1.1." *Durham University, Durham* 2011 (2011).
[18] Wang, Lin, Robin Quant and Athanasios Kolios. "Fluid structure interaction modelling of horizontal-axis wind turbine blades based on CFD and FEA." *Journal of Wind Engineering and Industrial Aerodynamics* 158 (2016): 11-25. https://doi.org/10.1016/j.jweia.2016.09.006
[19] Wang, Lin, Xinzi Tang and Xiongwei Liu. "Blade Design Optimisation for Fixed-Pitch Fixed-Speed Wind Turbines." *International Scholarly Research Notices* 2012, no. 1 (2012): 682859. https://doi.org/10.5402/2012/682859
[20] Zhu, Jie, Xiaohui Ni and Xiaomei Shen. "Aerodynamic and structural optimization of wind turbine blade with static aeroelastic effects." *International Journal of Low-Carbon Technologies* 15, no. 1 (2020): 55-64. https://doi.org/10.1093/ijlct/ctz057
[21] Shakya, Praveen, Matt Thomas, Abdennour C. Seibi, Mohammad Shekaramiz and MohammadA S. Masoum. "Fluid-structure interaction and life prediction of small-scale damaged horizontal axis wind turbine blades." *Results in Engineering* 23 (2024): 102388. https://doi.org/10.1016/j.rineng.2024.102388
[22] Paulsen, Uwe Schmidt, Helge Aagård Madsen, Jesper Henri Hattel, Ismet Baran and Per Hørlyck Nielsen. "Design optimization of a 5 MW floating offshore vertical-axis wind turbine." *Energy Procedia* 35 (2013): 22-32. https://doi.org/10.1016/j.egypro.2013.07.155

[23] Muskulus, Michael and Sebastian Schafhirt. "Design optimization of wind turbine support structures-a review." *Journal of Ocean and Wind Energy* 1, no. 1 (2014): 12-22.
[24] Tawade, Satishkumar V., Sachin B. Todkar, and Ashwinikumar S. Hade. "Fatigue life optimization of wind turbine blade." *International Journal of Research in Engineering and Technology* 3, no. 15 (2014): 843-850.
[25] Derakhshan, Shahram, Ali Tavaziani and Nemat Kasaeian. "Numerical shape optimization of a wind turbine blades using artificial bee colony algorithm." *Journal of Energy Resources Technology* 137, no. 5 (2015): 051210. https://doi.org/10.1115/1.4031043
[26] Jureczko, Mariola and Maciej Mrówka. "Multiobjective optimization of composite wind turbine blade." *Materials* 15, no. 13 (2022): 4649. https://doi.org/10.3390/ma15134649
[27] Peng, H. Y., M. N. Liu, H. J. Liu and K. Lin. "Optimization of twin vertical axis wind turbines through large eddy simulations and Taguchi method." *Energy* 240 (2022): 122560. https://doi.org/10.1016/j.energy.2021.122560
[28] Chen, Jin, Quan Wang, Wen Zhong Shen, Xiaoping Pang, Songlin Li and Xiaofeng Guo. "Structural optimization study of composite wind turbine blade." *Materials & Design (1980-2015)* 46 (2013): 247-255. https://doi.org/10.1016/j.matdes.2012.10.036
[29] Muhsen, Hani, Wael Al-Kouz and Waqar Khan. "Small wind turbine blade design and optimization." *Symmetry* 12, no. 1 (2019): 18. https://doi.org/10.3390/sym12010018
[30] Wind Turbine. "GE General Electric GE 1.5xle - 1,50 MW." (2013). https://en.wind-turbine-models.com/turbines/656-ge-general-electric-ge-1.5xle
[31] Schubel, Peter J. and Richard J. Crossley. "Wind turbine blade design." *Energies* 5, no. 9 (2012): 3425-3449. https://doi.org/10.3390/en5093425
[32] Air Foil Tools. "NREL's S818 Airfoil (s818-nr)." http://airfoiltools.com/airfoil/details?airfoil=s818-nr